

Phosphorylation of a WRKY Transcription Factor by Two Pathogen-Responsive MAPKs Drives Phytoalexin Biosynthesis in *Arabidopsis*

Guohong Mao,^{a,1} Xiangzong Meng,^a Yidong Liu,^a Zuyu Zheng,^{b,2} Zhixiang Chen,^b and Shuqun Zhang^{a,3}

^aDepartment of Biochemistry, Interdisciplinary Plant Group, and Bond Life Sciences Center, University of Missouri, Columbia, Missouri 65211

^bDepartment of Botany and Plant Pathology, Purdue University, West Lafayette, Indiana 47907

Plant sensing of invading pathogens triggers massive metabolic reprogramming, including the induction of secondary antimicrobial compounds known as phytoalexins. We recently reported that MPK3 and MPK6, two pathogen-responsive mitogen-activated protein kinases, play essential roles in the induction of camalexin, the major phytoalexin in *Arabidopsis thaliana*. In search of the transcription factors downstream of MPK3/MPK6, we found that WRKY33 is required for MPK3/MPK6-induced camalexin biosynthesis. In *wrky33* mutants, both gain-of-function MPK3/MPK6- and pathogen-induced camalexin production are compromised, which is associated with the loss of camalexin biosynthetic gene activation. WRKY33 is a pathogen-inducible transcription factor, whose expression is regulated by the MPK3/MPK6 cascade. Chromatin immunoprecipitation assays reveal that WRKY33 binds to its own promoter *in vivo*, suggesting a potential positive feedback regulatory loop. Furthermore, WRKY33 is a substrate of MPK3/MPK6. Mutation of MPK3/MPK6 phosphorylation sites in WRKY33 compromises its ability to complement the camalexin induction in the *wrky33* mutant. Using a phospho-protein mobility shift assay, we demonstrate that WRKY33 is phosphorylated by MPK3/MPK6 *in vivo* in response to *Botrytis cinerea* infection. Based on these data, we conclude that WRKY33 functions downstream of MPK3/MPK6 in reprogramming the expression of camalexin biosynthetic genes, which drives the metabolic flow to camalexin production in *Arabidopsis* challenged by pathogens.

INTRODUCTION

Plant recognition of pathogen-associated molecular patterns (PAMPs) or pathogen-derived effector proteins triggers massive changes in gene expression, cellular metabolism, and eventually induced resistance (Staskawicz et al., 1995; Dangl and Jones, 2001; Nürnberger and Scheel, 2001; Martin et al., 2003; Ausubel, 2005; Boller, 2005). One of the earliest signaling events after plant sensing of invading pathogens is the activation of mitogen-activated protein kinases (MAPKs) (Tena et al., 2001; Zhang and Klessig, 2001; Ichimura et al., 2002; Nakagami et al., 2005). *Arabidopsis thaliana* has three stress/pathogen-responsive MAPKs: MPK3, MPK6, and MPK4. MPK3 and MPK6 function together in a single MAPK cascade because they share common upstream kinases, are coactivated, and are functionally redun-

dant (Asai et al., 2002; Ren et al., 2002, 2008; Wang et al., 2008). MPK3 and MPK6 are orthologous to tobacco (*Nicotiana tabacum*) WIPK and SIPK, respectively (Zhang and Klessig, 2001; Ichimura et al., 2002; Ren et al., 2002). In tobacco, SIPK and WIPK share a common upstream MAPKK, Nt MEK2 (Yang et al., 2001). There are two Nt MEK2 orthologs in *Arabidopsis*, MKK4 and MKK5 (Ren et al., 2002). *Arabidopsis* MPK4 forms another independent MAPK cascade with upstream MKK1/MKK2 and MEKK1 (Petersen et al., 2000; Suarez-Rodriguez et al., 2007; Qiu et al., 2008a).

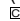
Loss- and gain-of-function studies provide genetic evidence supporting a positive role of the MPK3/MPK6 cascade in signaling plant disease resistance (Yang et al., 2001; Asai et al., 2002; Jin et al., 2003; Kroj et al., 2003; del Pozo et al., 2004; Menke et al., 2004; Beckers et al., 2009). Identification of the first plant MAPK substrate revealed that MPK3/MPK6 regulate ethylene production by phosphorylating a subset of ACC synthase (ACS) isoforms (Liu and Zhang, 2004; Joo et al., 2008; Han et al., 2010). Ethylene plays important roles in plant defense (Broekaert et al., 2006; van Loon et al., 2006). Recently, ERF104, an ethylene response factor, was shown to be a MPK6 substrate that plays important roles in plant resistance to a nonadapted bacterial pathogen (Bethke et al., 2009). The MPK3/MPK6 cascade is also involved in defense gene activation, reactive oxygen species generation, and hypersensitive response-like cell death (Ren et al., 2002; Kroj et al., 2003; Kim and Zhang, 2004; Liu et al., 2007). The importance of MAPK signaling in plant-pathogen

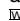
¹Current address: Donald Danforth Plant Science Center, 975 North Warson Road, St. Louis, MO 63132.

²Current address: Salk Institute for Biological Studies, 10010 North Torrey Pines Road, La Jolla, CA 92036.

³Address correspondence to zhangsh@missouri.edu.

The author responsible for distribution of materials integral to the findings presented in this article in accordance with the policy described in the Instructions for Authors (www.plantcell.org) is: Shuqun Zhang (zhangsh@missouri.edu).

Some figures in this article are displayed in color online but in black and white in the print edition.

Online version contains Web-only data.

www.plantcell.org/cgi/doi/10.1105/tpc.111.084996

interactions is also supported by studies of bacterial effectors, several of which target plant MAPK cascades (Zhang et al., 2007; Cui et al., 2010).

Induction of antimicrobial phytoalexins is an integral part of plant disease resistance (VanEtten et al., 1989; Hammerschmidt, 1999; Dixon, 2001). Evidence supporting a positive role of phytoalexins in plant disease resistance comes from studies of both pathogens and plants. Disruption of pathogen genes that encode enzymes known to detoxify phytoalexins can lead to loss of pathogenicity, and the virulence of a pathogen on a specific host sometimes coevolves with the generation of enzymes that are capable of degrading plant phytoalexins (VanEtten et al., 1989; Morrissey and Osbourn, 1999). In addition, mutations of plant genes in the phytoalexin biosynthetic and regulatory pathways, which result in reduced phytoalexin biosynthesis, can lead to increased susceptibility of plants to pathogens (Thomma et al., 1999; Ferrari et al., 2003, 2007; Nafisi et al., 2007; Ren et al., 2008). In recent years, the biosynthetic pathways of a number of phytoalexins have been fully elucidated, and it has been demonstrated that phytoalexin induction is associated with the activation of genes encoding enzymes in the biosynthetic pathways (Hammerschmidt, 1999; Dixon, 2001). However, the signal transduction pathway(s) leading to the activation of these genes are mostly unclear.

We previously reported that the pathogen-responsive MPK3/MPK6 cascade plays a positive role in regulating the biosynthesis of camalexin (3-thiazol-2'-yl-indole; Tsuji et al., 1992), the major phytoalexin in *Arabidopsis* (Ren et al., 2008). Activation of the MPK3/MPK6 cascade leads to coordinated upregulation of multiple genes encoding enzymes in the camalexin biosynthetic pathway, including CYP71A13, which converts indole-3-acetaldoxime to indole-3-acetonitrile, and PAD3, which encodes another P450 enzyme (CYP71B15) that carries out the last step of camalexin biosynthesis (Zhou et al., 1999; Schuegger et al., 2006; Nafisi et al., 2007; Böttcher et al., 2009). We also hypothesized that MPK3/MPK6 are likely to phosphorylate a transcription factor or factors, which is/are directly responsible for activating the expression of camalexin biosynthetic genes (Ren et al., 2008).

In our search for the transcription factor(s) downstream of MPK3/MPK6 in *Arabidopsis* or their orthologous WIPK/SIPK in tobacco, we identified WRKY transcription factors, including *Arabidopsis* WRKY33, as potential downstream targets based on their gene activation in the gain-of-function GVG-Nt-MEK2^{DD} plants (Kim and Zhang, 2004; Wan et al., 2004). Later, it was shown that WRKY33 expression is highly induced in *Arabidopsis* treated with PAMPs or infected by pathogens and that *wrky33* mutants are more susceptible to *Botrytis cinerea* and to *Alternaria brassicicola* (Zheng et al., 2006; Lippok et al., 2007). In the same studies, it was also demonstrated that WRKY33 is nuclear localized and that it binds to the W-box *cis*-element. More recently, WRKY33 was shown to be essential for the induction of camalexin biosynthesis in *Arabidopsis* infected with *Pseudomonas syringae*, and WRKY33 directly binds to the PAD3 promoter (Qiu et al., 2008b).

In this report, we demonstrate that the WRKY33 transcription factor functions downstream of MPK3/MPK6 in activating the expression of camalexin biosynthetic genes. In the *wrky33* mutant background, both the gain-of-function MPK3/MPK6-

and *B. cinerea*-induced camalexin production are compromised, which is associated with the loss of activation of camalexin biosynthetic genes. WRKY33 is a pathogen-inducible transcription factor, whose expression is regulated by the MPK3/MPK6 cascade. In addition, WRKY33 is a substrate of MPK3/MPK6. Using a phospho-protein mobility shift assay, we show that WRKY33 is phosphorylated by MPK3/MPK6 in vivo in response to *B. cinerea* infection. Furthermore, mutation of MPK3/MPK6 phosphorylation sites in WRKY33 compromises its ability to complement the deficiency of camalexin induction in the *wrky33* mutant. These results demonstrate that WRKY33 acts downstream of MPK3/MPK6 in reprogramming the expression of camalexin biosynthetic genes, which drives the metabolic flow to camalexin production in *Arabidopsis* infected by pathogens.

RESULTS

WRKY33 Is Essential for Gain-of-Function GVG-Nt-MEK2^{DD}- and *B. cinerea*-Induced Camalexin Biosynthesis

Using a gel mobility shift assay, we identified WRKY transcription factors as potential targets of SIPK/WIPK in tobacco defense response (Kim and Zhang, 2004). To identify the specific WRKY(s) involved, we took a genetic approach in *Arabidopsis* by crossing the dexamethasone (DEX)-inducible promoter-driven constitutively active Nt MEK2^{DD} transgene (GVG-Nt-MEK2^{DD}, abbreviated as DD) (Yang et al., 2001; Ren et al., 2002) into different *wrky* mutant backgrounds. Our initial efforts were focused on WRKY members, including WRKY6, WRKY33, WRKY40, and WRKY53, whose expressions are induced in the DD plants after DEX treatment (Wan et al., 2004) (Y. Liu and S. Zhang, unpublished data). Known MPK3/MPK6-regulated defense responses, including defense gene activation, ethylene induction, and camalexin production (Kim and Zhang, 2004; Liu and Zhang, 2004; Ren et al., 2008), were monitored in the DD/*wrky* double mutants. As shown in Figure 1A, DD-induced camalexin production was blocked in the *wrky33*, but not *wrky6*, *wrky40*, or *wrky53*, background, suggesting that WRKY33 is downstream of MPK3/MPK6 in regulating camalexin biosynthesis. DD expression and MPK3/MPK6 activation after DEX treatment were not affected in the DD/*wrky33* double mutant (Figure 1B). Compromised camalexin induction was associated with the loss of activation of camalexin biosynthetic genes, including CYP71A13 and PAD3 (Figures 1C and 1D), consistent with our previous report that gene activation is involved in MPK3/MPK6-induced camalexin biosynthesis (Ren et al., 2008).

Two *wrky33* mutant alleles were analyzed, which gave similar results. In addition, we transformed a WRKY33 native promoter driven tandem-affinity purification (TAP)-tagged WRKY33 construct (WRKY33-TAP) into the DD/*wrky33* background. As shown in Figure 1E, this construct fully rescued camalexin induction in the DD/*wrky33* plants. Again, the induction of the DD protein and the MPK3/MPK6 activation were the same in plants with different genotypes (Figure 1F, top and middle). Previously, we reported that WRKY33 expression is highly induced by MPK3/MPK6 activation (Wan et al., 2004). With the

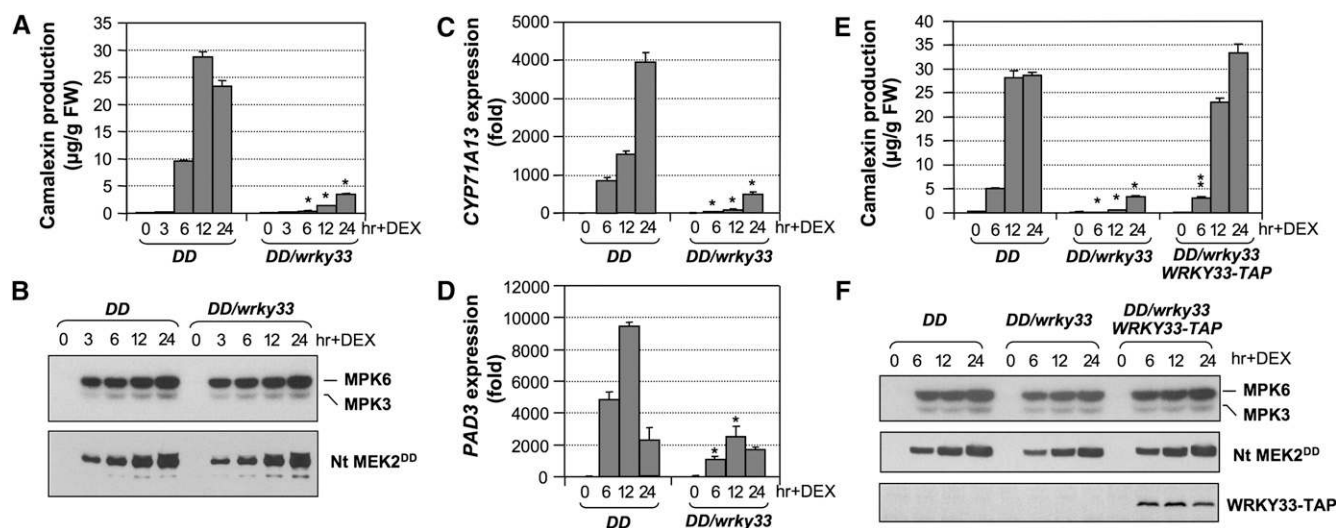


Figure 1. Induction of Camalexin Biosynthesis in the Gain-of-Function *GVG-Nt-MEK2^{DD}* Transgenic Plants (*DD*) Is Dependent on the *WRKY33* Transcription Factor.

(A) Mutation of *WRKY33* inhibited camalexin biosynthesis in *DD* seedlings. Two-week-old *DD* and *DD/wrky33* seedlings were treated with DEX (1 μ M final concentration). Camalexin accumulation was measured at indicated times. Error bars indicate SE ($n = 3$). FW, fresh weight.

(B) Normal *DD* induction (bottom) and MPK3/MPK6 activation (top) in *DD/wrky33* seedlings. Flag-tagged *DD* protein was detected by immunoblot analysis using an anti-Flag antibody. MPK6 and MPK3 activation were determined by an in-gel kinase assay using MBP as a substrate.

(C) and (D) Activation of camalexin biosynthetic genes, including *CYP71A13* (C) and *PAD3* (D), was compromised in the *wrky33* background. Transcript levels were determined by real-time qPCR. Error bars indicate SE ($n = 3$).

(E) Complementation of *wrky33* mutation by a native *WRKY33* promoter-driven *WRKY33-TAP* construct. Error bars indicate SE ($n = 3$).

(F) Induction of *WRKY33-TAP* protein in *DD/WRKY33-TAP/wrky33* plants after MPK3/MPK6 activation. Total protein extracts prepared from seedlings shown in (E) were subjected to an in-gel kinase assay using MBP as a substrate (top), and immunoblot analyses using anti-Flag antibody to detect Flag-tagged *DD* protein (middle) and anti-IgG-HRP conjugate to detect the TAP-tagged *WRKY33* (bottom). Statistically different data groups at a specific time point (P value < 0.05) are indicated using different numbers of asterisks (0 to 2) vertically placed above the columns in the graphs.

TAP tag, we examined the *WRKY33* protein levels before and after MPK3/MPK6 activation. As shown in Figure 1F (bottom), the *WRKY33* protein was undetectable before MPK3/MPK6 activation and accumulated to high levels after MPK3/MPK6 activation, consistent with the activation of *WRKY33* gene expression in *DD* plants after DEX treatment (Wan et al., 2004).

WRKY33 is also essential for *B. cinerea*-induced camalexin biosynthesis. Camalexin induction in the *wrky33* mutants was compromised (Figure 2A), which was associated with the greatly reduced activation of *CYP71A13* and *PAD3* gene expression (Figures 2C and 2D). The activation of MPK3/MPK6 was not affected in the *wrky33* mutants (Figure 2B), consistent with a function of *WRKY33* downstream of MPK3/MPK6. The *WRKY33-TAP* transgene fully rescued the deficiency of *wrky33* at 24 h after *B. cinerea* inoculation (Figure 2E). Again, the *WRKY33-TAP* protein was absent before pathogen infection and was induced by *B. cinerea* infection (Figure 2F), which was associated with the activation *WRKY33* at transcriptional level (see Supplemental Figure 1 online).

The Pathogen-Responsive MPK3/MPK6 Cascade Is Involved in *WRKY33* Gene Activation

WRKY33 is a PAMP/pathogen-responsive WRKY transcription factor that is essential to *B. cinerea* resistance (Zheng et al.,

2006; Lippok et al., 2007). Gain-of-function activation of MPK3/MPK6 is sufficient to activate *WRKY33* expression (Wan et al., 2004), suggesting that the MPK3/MPK6 cascade might be involved in PAMP/pathogen-induced *WRKY33* gene activation. To provide loss-of-function evidence, we examined *WRKY33* expression in *B. cinerea*-infected wild type (Columbia-0 [Col-0]), single *mpk3* or *mpk6* mutants, and the rescued *mpk3 mpk6* double mutant (Wang et al., 2007; Ren et al., 2008). The conditionally rescued *mpk3 mpk6* double mutant was obtained by transforming a DEX-inducible promoter-driven *MPK6* (*GVG-MPK6*) into *mpk3^{-/-}/mpk6^{+/-}* plants. When the T3 *mpk3^{-/-}/mpk6^{+/-}/GVG-MPK6^{+/+}* plants began to flower, DEX was sprayed every other day to rescue the embryo lethality of the *mpk3^{-/-}/mpk6^{-/-}/GVG-MPK6^{+/+}* zygotes. Progenies with *mpk3^{-/-}/mpk6^{-/-}/GVG-MPK6^{+/+}* genotype, which still show developmental defects (Wang et al., 2007), were called rescued *mpk3 mpk6* double mutants and were used for experiments.

As shown in Figure 3A, *WRKY33* activation was not affected in the single *mpk3* or *mpk6* mutants. However, in the rescued *mpk3 mpk6* double mutant, *WRKY33* induction was compromised and much delayed, suggesting that the MPK3/MPK6 cascade is required for full induction of *WRKY33* expression. The residual activation of *WRKY33* in the *mpk3 mpk6* double mutant suggests that other pathways are also involved in *B. cinerea*-induced *WRKY33* expression. It is also possible that the basal level

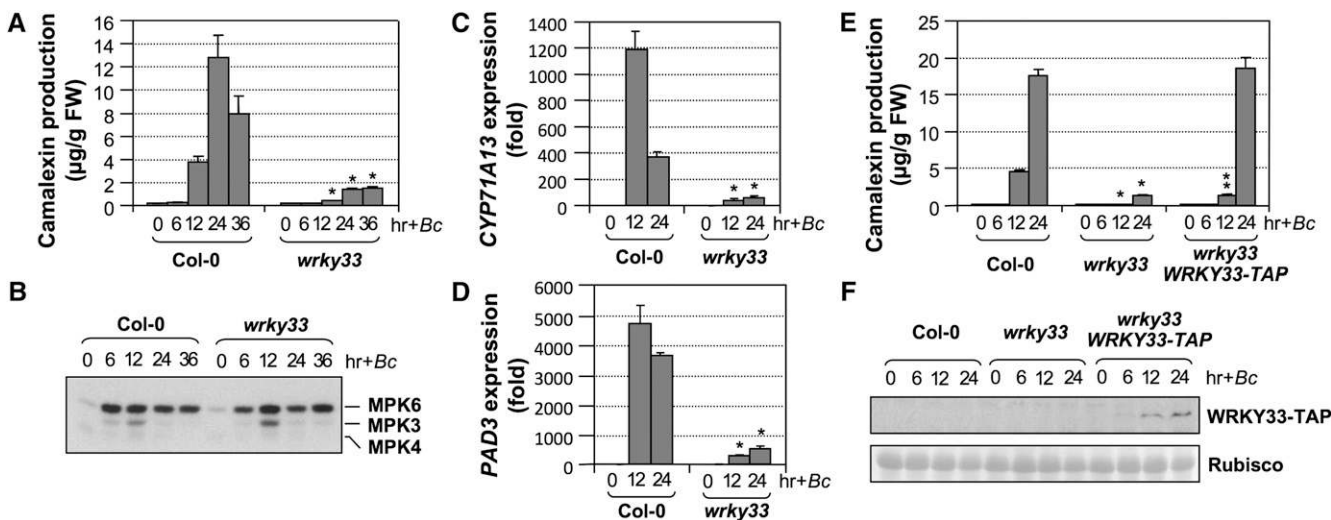


Figure 2. WRKY33 Is Essential to Camalexin Induction in *Arabidopsis* after *B. cinerea* Infection.

(A) Mutation of *WRKY33* compromised *B. cinerea*-induced camalexin biosynthesis. Two-week-old wild-type (Col-0) and *wrky33* seedlings were inoculated with *B. cinerea* spores, and camalexin accumulation was measured at indicated times. Error bars indicate SE ($n = 3$). FW, fresh weight.

(B) MPK3/MPK6 activation in the *wrky33* mutant was not affected. MAPK activation in these seedlings was determined by an in-gel kinase assay using MBP as a substrate.

(C) and **(D)** Activation of camalexin biosynthetic genes, including *CYP71A13* **(C)** and *PAD3* **(D)**, was compromised in the *wrky33* mutant. Transcript levels were determined by real-time qPCR. Error bars indicate SE ($n = 3$).

(E) Complementation of *wrky33* mutation by a native *WRKY33* promoter-driven *WRKY33-TAP* construct. Error bars indicate SE ($n = 3$).

(F) Induction of *WRKY33-TAP* protein in *WRKY33-TAP/wrky33* plants by *B. cinerea*. Total protein extracts prepared from seedlings shown in **(E)** were subjected to immunoblot analyses using a goat anti-IgG-HRP conjugate to detect the TAP-tagged *WRKY33* (top). Equal amounts (10 μ g) were loaded to each lane and were confirmed by Ponceau S staining (bottom). Statistically different data groups at a specific time point (P value < 0.05) are indicated using different numbers of asterisks (0 to 2) vertically placed above the columns in the graphs.

expression of the *GVG-MPK6* transgene might be able to compensate the mutant to a certain extent, although this is unlikely since we detected little/no activity from the transgenic *MPK6* by the in-gel kinase activity assay in the rescued *mpk3 mpk6* double mutant after *B. cinerea* infection (Ren et al., 2008; Han et al., 2010).

In Vitro Phosphorylation of WRKY33 by MPK3 and MPK6

Despite a partial blockage of *WRKY33* gene activation, camalexin induction in the *mpk3 mpk6* double mutant was almost completely inhibited (Ren et al., 2008). Associated with it, induction of *CYP71A13* and *PAD3* expression was also abolished (Figures 3B and 3C). This result suggests that MPK3/MPK6 might regulate *WRKY33* at additional levels. It is possible that phosphorylation by MPK3/MPK6 is required to fully activate the de novo synthesized *WRKY33* protein. In the absence of MPK3 and MPK6, residual induction of *WRKY33* is unable to fully activate the expression of downstream camalexin biosynthetic genes, resulting in compromised camalexin induction. An examination of *WRKY33* protein sequence revealed a cluster of five potential MAPK phosphorylation sites (Ser-54, Ser-59, Ser-65, Ser-72, and Ser-85) in the N terminus of the *WRKY33* protein (Figure 4A). As a result, we prepared a His-tagged recombinant *WRKY33* protein for in vitro MAPK phosphorylation assays.

As shown in Figure 4B (top), activated recombinant MPK3 and MPK6 strongly phosphorylated *WRKY33*. By contrast, MPK10, a

closely related homolog of MPK3 and MPK6, failed to do so. All three MAPKs were able to phosphorylate myelin basic protein (MBP), demonstrating that all were active (Figure 4B, bottom). Without activation by the constitutively active *MKK4^{DD}/MKK5^{DD}*, neither MPK3 nor MPK6 was able to phosphorylate *WRKY33* (Figure 4B), confirming the importance of phosphorylation activation of MPK3/MPK6 by its upstream *MKK4/MKK5*. In the autoradiogram, the phosphorylation labeling of MAPKs by *MKK4^{DD}/MKK5^{DD}* was evident (Figure 4B, top). When all five Ser residues were mutated to Ala (*WRKY33^{SA}*), the protein could no longer be phosphorylated by MPK3/MPK6 (Figure 4C).

In addition to recombinant MAPKs, we also analyzed the phosphorylation of *WRKY33* by the native MAPKs. In this assay, recombinant *WRKY33^{WT}* or *WRKY33^{SA}* protein was embedded in an SDS-PAGE gel instead of MBP. Phosphorylation of the embedded *WRKY33* was determined by an in-gel kinase assay using total protein extracts from Col-0, *mpk3*, *mpk6*, and *mpk3 mpk6* seedlings treated with *B. cinerea*, which activates MPK3/MPK6 and MPK4 cascades (Ren et al., 2008; Han et al., 2010). As shown in Figure 4D, identical kinase activity patterns were observed when *WRKY33^{WT}* and MBP were used as the substrates. By contrast, no kinase activity was detected when *WRKY33^{SA}* was embedded in the gel. The loss of kinase bands in their respective mutants confirmed the MAPK identities. In addition to MPK3 and MPK6, we also detected the activity of MPK4 in assays using *WRKY33^{WT}* and MBP (but not *WRKY33^{SA}*)

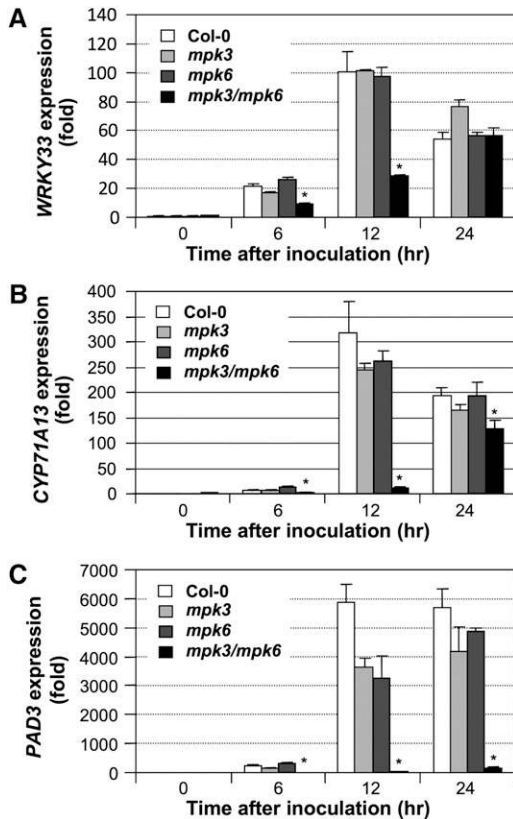


Figure 3. *WRKY33* Induction after *B. cinerea* Infection Is Dependent on the MPK3/MPK6 Cascade.

(A) Induction of *WRKY33* gene expression was compromised in the rescued *mpk3 mpk6* double mutant. Wild-type (Col-0), *mpk3*, *mpk6*, and *mpk3 mpk6* seedlings were inoculated with *B. cinerea*. Samples were collected at indicated times. Induction of the *WRKY33* transcript was quantified by real-time qPCR. Error bars indicate SE ($n = 3$).

(B) and (C) Activation of camalexin biosynthetic genes, including *CYP71A13* (B) and *PAD3* (C), was compromised in the *mpk3 mpk6* mutant. Error bars indicate SE ($n = 3$). Asterisks above the columns indicate the data sets that are statistically different from those without asterisk at a specific time point (P value < 0.05).

as substrates, suggesting that MPK4 is able to phosphorylate *WRKY33* in vitro on the same Ser residues. Similar to our previous reports (Ren et al., 2008; Han et al., 2010), higher levels of MPK4 activity were observed in the *mpk3 mpk6* double mutant after *B. cinerea* infection (Figure 4D). This could be a result of higher MPK4 protein levels in the *mpk3 mpk6* double mutant (Han et al., 2010). It is also possible that MPK4 cascade and MPK3/MPK6 cascade share common upstream components after the sensing of *B. cinerea*. The loss of MPK3/MPK6 cascade leads to a higher signaling strength feeding into the MPK4 cascade.

MPK3/MPK6 Phosphorylation Sites in *WRKY33* Are Essential for Its Full Activity in Vivo

To determine the importance of *WRKY33* phosphorylation by MPK3/MPK6 in vivo, we investigated the ability of *WRKY33^{SA}* in

complementing the *wrky33* mutant phenotype. In this experiment, we used the constitutive 35S promoter-driven *WRKY33^{WT}* and *WRKY33^{SA}* constructs so that the regulation of *WRKY33* at the phosphorylation level by MPK3/MPK6 could be studied separately from its regulation at the transcriptional level. A four-copy myc tag (4myc) was added to the N terminus for easy detection of the *WRKY33* protein. More than 30 independent lines of each construct were analyzed to determine the induction of camalexin production after *B. cinerea* infection. We found that *WRKY33^{SA}* lines had lower levels of camalexin induction than *WRKY33^{WT}* lines with similar levels of expression, and none of the *WRKY33^{SA}* lines showed full rescue of the *wrky33*

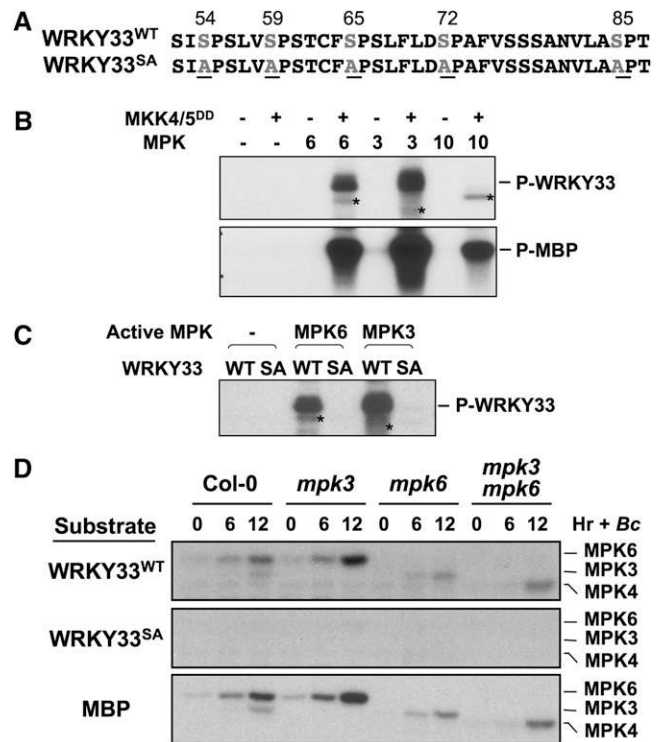


Figure 4. In Vitro Phosphorylation of *WRKY33* by MPK3 and MPK6.

(A) Putative MAPK phosphorylation sites in the N terminus of *WRKY33* and the loss-of-phosphorylation *WRKY33* mutant with all five Ser mutated to Ala (*WRKY33^{SA}*).

(B) Phosphorylation of *WRKY33* in vitro by the activated MPK3 and MPK6 but not MPK10. Reactions with various components omitted (–) were used as controls. The asterisks in the top panel indicate the phosphorylation of MAPKs by MKK4^{DD}/MKK5^{DD}.

(C) Mutation of MAPK phosphorylation sites abolished the phosphorylation of *WRKY33* by MPK3 and MPK6. Recombinant *WRKY33^{WT}* (WT) and *WRKY33^{SA}* (SA) were incubated with activated MPK3 and MPK6 as in (B). Phosphorylated *WRKY33* was visualized by autoradiography after gel electrophoresis.

(D) Phosphorylation of *WRKY33^{WT}*, but not *WRKY33^{SA}*, by the native MAPKs extracted from seedlings treated with *B. cinerea*. Total extracts were prepared from wild-type (Col-0), *mpk3*, *mpk6*, and *mpk3 mpk6* seedlings infected with *B. cinerea*. MAPK activities were detected by an in-gel kinase assay using recombinant *WRKY33^{WT}* (top), recombinant *WRKY33^{SA}* (middle), and MBP (bottom) as substrates.

mutant. The highest level of rescue was ~50% at 24 h after inoculation (Figure 5A). By contrast, many *WRKY33^{WT}*-rescued lines were obtained. Examination of *WRKY33* protein levels revealed that even the lines with partial complementation expressed *WRKY33^{SA}* at a higher level than the *WRKY33^{WT}* line with full rescue (Figures 5A and 5B). This result revealed that *WRKY33^{SA}* was less efficient in complementing the *wrky33* mutant. The higher *WRKY33^{SA}* protein level was associated with a higher level of gene expression (Figure 5C). In the wild-type (Col-0) control, induction of *WRKY33* expression was evident. In both transgenic lines, transcripts were constitutively expressed because of the 35S promoter. In the vector/*wrky33* control, no *WRKY33* transcript was detectable, demonstrating the specificity of the RT-PCR reaction. RT-PCR with a primer pair that spans the whole open reading frame was used to examine *WRKY33* transgene expression in the *wrky33* background because *wrky33* mutant alleles still produce nonfunctional transcripts (Zheng et al., 2006). We tried several pairs of quantitative PCR (qPCR) primers, and all of them amplified the cDNAs from the mutated gene transcripts. We found that the native promoter driven *WRKY33^{SA}* construct also failed to fully complement the camalexin induction in the *wrky33* mutant background (see Supplemental Figure 2 online).

Loss-of-phosphorylation mutant *WRKY33^{SA}* was also less efficient in complementing the activation of camalexin biosynthetic genes in the *wrky33* mutant (Figures 5D and 5E). The induction of *CYP71A13* and *PAD3* gene expression was much lower at 12 h after *B. cinerea* inoculation in the *WRKY33^{SA}*/*wrky33* seedlings in comparison to that in the wild-type control (Col-0) and *WRKY33^{WT}*/*wrky33* seedlings. The much-delayed induction of camalexin biosynthetic genes is likely to hamper the accumulation enzyme activities, resulting in the lower camalexin production in *WRKY33^{SA}*/*wrky33* seedlings (Figure 5A). Once the cell death sets in at the later stage of the infection process, the cell will eventually have a reduced metabolic capacity and may lose the ability to produce camalexin.

To determine the importance of *WRKY33* phosphorylation in camalexin induction in the gain-of-function *DD* plants, we crossed the transgenic lines shown in Figure 5A (homozygous vector/*wrky33*, *WRKY33^{WT}*/*wrky33*, and *WRKY33^{SA}*/*wrky33*) with *DD*/*wrky33* to generate *DD*/vector/*wrky33*, *DD*/*WRKY33^{WT}*/*wrky33*, and *DD*/*WRKY33^{SA}*/*wrky33*. Large numbers of crosses were performed to obtain enough F1 seeds for experiments. They were homozygous for *wrky33* and heterozygous for *DD* and *WRKY33^{WT}* or *WRKY33^{SA}*. Camalexin accumulation after DEX treatment in these lines was compared. As shown in Figure 6A, *WRKY33^{WT}* was able to fully complement the loss of endogenous *WRKY33*. However, *WRKY33^{SA}* could only partially rescue *wrky33*. Immunoblot analysis using an anti-myc antibody revealed that *WRKY33^{SA}* expressed at a higher level than *WRKY33^{WT}* (Figure 6B), ruling out the possibility that the partial complementation by the *WRKY33^{SA}* transgene was a result of lower expression. Again, the lower efficiency of *WRKY33^{SA}* in complementing the *DD*-induced camalexin production in the *wrky33* mutant (Figure 6A) was associated with the compromised induction of camalexin biosynthetic genes, including *CYP71A13* and *PAD3* (Figures 6C and 6D). Based on these data, we can conclude that *WRKY33^{SA}*, a loss-of-phosphorylation mutant, cannot achieve the

full activity of *WRKY33^{WT}* in activating the expression of camalexin biosynthetic genes, highlighting the importance of *WRKY33* phosphorylation by MPK3/MPK6 in camalexin induction.

Phosphorylation of *WRKY33* by MPK3/MPK6 in Vivo

The genetic evidence above demonstrates that MPK3/MPK6 phosphorylation sites in the N terminus of *WRKY33* are important for the full induction of camalexin biosynthesis in plants challenged by *B. cinerea* or in the gain-of-function *DD* plants (Figures 5 and 6). To provide direct evidence that *WRKY33* is phosphorylated by MPK3/MPK6 in vivo, we used the Phos-tag mobility shift assay, in which the binding of phospho-proteins to the Phos-tag reagent in the SDS-PAGE gel matrix slows down their movement (Bethke et al., 2009). Protein extracts from *WRKY33^{WT}*/*wrky33* and *WRKY33^{SA}*/*wrky33* plants treated with *B. cinerea* were first separated in a Phos-tag SDS-PAGE gel, and 4myc-tagged *WRKY33* was detected by immunoblot analysis. Extracts from the wild type (Col-0) were used as a negative control to determine the specificity of the anti-myc immunoblot analysis. As shown in Figure 7A, upshift of 4myc-tagged *WRKY33^{WT}* was observed after *B. cinerea* infection, which was associated with a decrease in unphosphorylated *WRKY33^{WT}* protein. Such upshift was absent in the extracts from *WRKY33^{SA}*/*wrky33* plants, demonstrating the phosphorylation of *WRKY33* on the five MAPK phosphorylation sites after *B. cinerea* infection. Total 4myc-tagged *WRKY33* proteins were determined by regular immunoblot (Figure 7A, middle). Equal loading of protein was double confirmed by staining of nitrocellulose membrane with Ponceau S (Figure 7A, bottom).

To demonstrate the phosphorylation of *WRKY33* by MPK3/MPK6, we analyzed the phosphorylation status of *WRKY33* in the *DD* background. Protein extracts from *DD*, *DD*/*WRKY33^{WT}*/*wrky33*, and *DD*/*WRKY33^{SA}*/*wrky33* plants treated with DEX for different times were subjected to Phos-tag mobility shift assays. Within 6 h after DEX treatment, the majority of the *WRKY33^{WT}* protein was phosphorylated, as indicated by the upshift of the 4myc-tagged *WRKY33*. Associated with this, the amount of unphosphorylated protein decreased (Figure 7B, top). By contrast, no such upshift of *WRKY33^{SA}* was observed, demonstrating again that the phosphorylation was on the MAPK phosphorylation sites. Based on these data, we conclude that *WRKY33* is phosphorylated after MPK3/MPK6 activation and that the phosphorylation is dependent on the MAPK phosphorylation sites in the N terminus of *WRKY33*. Combined with the genetic evidence that the MPK3/MPK6 phosphorylation sites are required for the complementation of the *wrky33* mutant phenotype, we can conclude that MPK3/MPK6 phosphorylation of *WRKY33* is important to the activation of camalexin biosynthetic genes.

MPK3/MPK6 Phosphorylation of *WRKY33* Does Not Alter Its DNA Binding Activity

Phosphorylation of a transcription factor by a kinase may change the DNA binding activity of the transcription factor. To determine whether phosphorylation of *WRKY33* by MPK3/MPK6 alter its W-box binding activity, we performed an electrophoresis mobility shift assay (EMSA). As shown in Figure 8, wild-type *WRKY33*

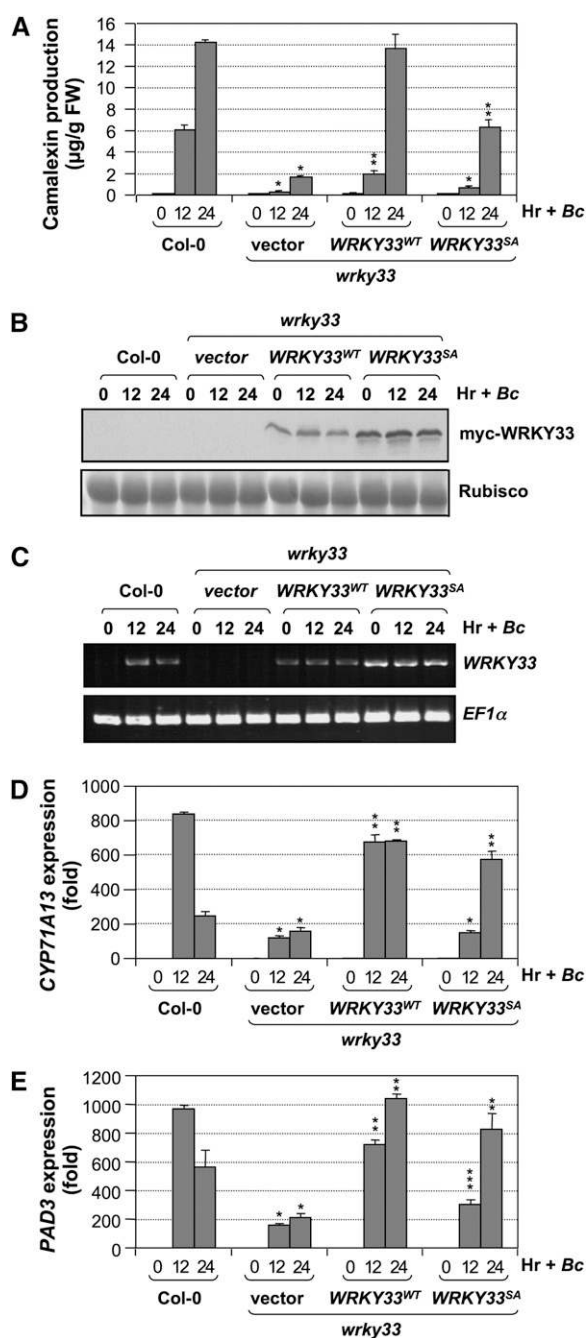


Figure 5. MPK3/MPK6 Phosphorylation Sites in WRKY33 Are Important for Its Function in Vivo.

(A) Loss-of-phosphorylation WRKY33 can only partially complement the *wrky33* mutant. Myc epitope-tagged WRKY33^{WT} and WRKY33^{SA} under the control of the constitutive 35S promoter were transformed into the *wrky33* mutant. An empty vector was used as a negative control. Camalexin accumulation was determined at indicated times after *B. cinerea* inoculation, and seedlings were collected for protein and RNA preparations. Error bars indicate SE ($n = 3$). FW, fresh weight.

(B) Expression of WRKY33^{SA} at a higher level despite a lower level of complementation. Levels of WRKY33 protein in samples collected in **(A)** were determined by immunoblot analysis using an anti-myc epitope

(WRKY33^{WT}) and loss-of-phosphorylation WRKY33 mutant (WRKY33^{SA}) had similar DNA binding activity to W-box. Inclusion of unlabeled W-box, but not GCC-box or as-1 box, in the binding reaction effectively competed the binding of WRKY33 to the ³²P-labeled W-box probe, demonstrating the specificity of W-box binding activity of WRKY33 protein. This experiment also demonstrated that the mutation of the five Ser residues in the MPK3/MPK6 phosphorylation sites to Ala residues does not interfere with the DNA binding activity of WRKY33.

To determine the effect of MPK3/MPK6 phosphorylation on the DNA binding activity of WRKY33, we first phosphorylated WRKY33 using the activated MPK3/MPK6. Since both MPK3 and MPK6 phosphorylate WRKY33 on the same sites (Figure 4), we used an equal mixture of MPK3 and MPK6 as the enzyme. A control reaction without the addition of MPK3/MPK6 was set side-by-side, which was used as unphosphorylated WRKY33. EMSA revealed no difference in the W-box binding activity between the phosphorylated WRKY33 and unphosphorylated WRKY33 (Figure 8B). This finding suggests that the phosphorylation of WRKY33 by MPK3/MPK6 might affect the transactivation activity rather than the W-box binding activity of WRKY33. This is consistent with the fact that MPK3/MPK6 phosphorylation sites in WRKY33 are far away from the DNA binding domain (Zheng et al., 2006), making it unlikely that the phosphorylation will change its DNA binding activity. In addition, we found that WRKY33 is constitutively associated with the chromatin since extraction buffer without SDS was unable to extract WRKY33 from cells.

Binding of WRKY33 to Its Own Promoter Suggests Potential Self-Activation of Transcription

Increase in the levels of WRKY33 protein, which is associated with *WRKY33* gene activation (Figures 1F, 2F, and 3A), is likely to play an important role in the activation of downstream genes during plant defense response. It was demonstrated that a cluster of W-box in the promoter of *WRKY33* is involved in the *WRKY33* gene activation in plants infected by pathogens or after PAMP treatment (Lippok et al., 2007). Furthermore, it was shown in the same report that WRKY transcription factors interact with these W-boxes in vivo based on chromatin immunoprecipitation (ChIP) assay. However, since an antibody against all/most WRKY

antibody (top). Equal loading was confirmed by Ponceau S staining (bottom).

(C) Higher WRKY33^{SA} protein levels were associated with higher transcript levels. Levels of *WRKY33* transcript in samples collected in **(A)** were examined by RT-PCR using a primer pair that did not amplify *WRKY33* with the T-DNA insertion (top). *EF1α* was used to show equal inputs of cDNA templates (bottom). Twenty-five cycles of PCR were performed.

(D) and **(E)** WRKY33^{SA} is less efficient in supporting the *B. cinerea*-induced activation of camalexin biosynthetic genes, including *CYP71A13* **(D)** and *PAD3* **(E)**. Transcript levels were determined by real-time qPCR. Error bars indicate SE ($n = 3$). Statistically different data groups at a specific time point (P value < 0.05) are indicated using different numbers of asterisks (0 to 3) vertically placed above the columns in the graphs.

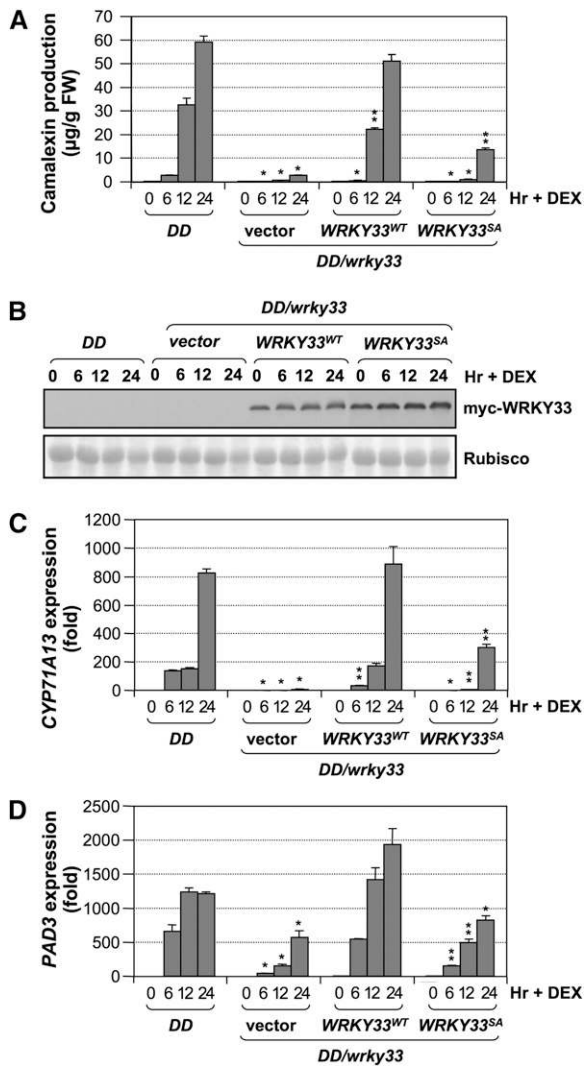


Figure 6. MPK3/MPK6 Phosphorylation Sites in WRKY33 Are Also Required for Camalexin Induction in the Gain-of-Function *DD* Seedlings.

(A) Loss-of-phosphorylation WRKY33 can only partially complement the camalexin induction in *DD/wrky33* mutant. The same transgenic lines shown in Figure 5 were crossed to *DD/wrky33* lines to generate *DD/wrky33/4myc-WRKY33^{WT}*, *DD/wrky33/4myc-WRKY33^{SA}*, and vector control lines. Camalexin accumulation was monitored at indicated times after DEX (1 μ M) treatment, and seedlings were collected for protein preparations. Error bars indicate SE ($n = 3$).

(B) Partial complementation by WRKY33^{SA} was not a result of a lower expression level. Levels of WRKY33 protein in the transgenic lines were determined in samples collected in **(A)** using an anti-myc antibody (top). Equal loading was confirmed by Ponceau S staining (bottom).

(C) and **(D)** WRKY33^{SA} is less efficient in supporting the MPK3/MPK6-induced activation of camalexin biosynthetic genes, including *CYP71A13* **(C)** and *PAD3* **(D)**. Transcript levels were determined by real-time qPCR. Error bars indicate SE ($n = 3$). Statistically different data groups at a specific time point (P value < 0.05) are indicated using different numbers of asterisks (0 to 2) vertically placed above the columns in the graphs.

transcription factors was used in the ChIP assay, the identity of the WRKY remains unknown. To determine whether WRKY33 is involved in regulating its own expression, we performed ChIP-qPCR assay to see whether WRKY33 binds to its own promoter. As shown in Figure 9A, *WRKY33* promoter was greatly enriched with an anti-myc antibody that immunoprecipitates the 4myc-tagged *WRKY33* transgene product. By contrast, IgG control failed to pull down *WRKY33* promoter DNA.

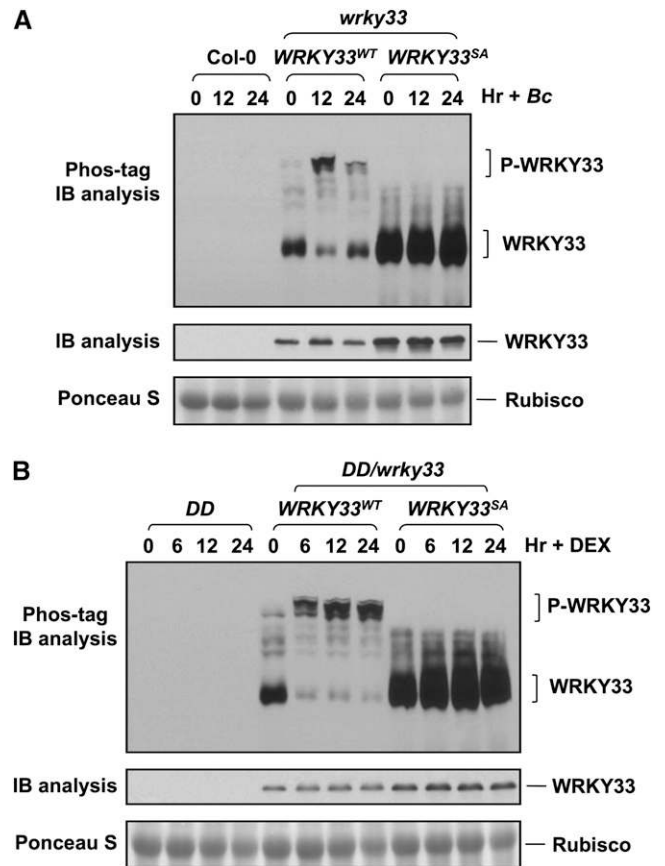


Figure 7. In Vivo Phosphorylation of WRKY33 by MPK3/MPK6.

(A) WRKY33 becomes phosphorylated in seedlings infected with *B. cinerea*. Protein extracts from wild-type (Col-0), *wrky33/4myc-WRKY33^{WT}*, and *wrky33/4myc-WRKY33^{SA}* seedlings treated with *B. cinerea* for different times were separated in an SDS-PAGE gel with Phos-tag reagent. After being transferred to a nitrocellulose membrane, myc-tagged WRKY33^{WT} and WRKY33^{SA} proteins were detected by an anti-myc antibody (top). A regular immunoblot (IB) was done at the same time to detect total WRKY33 protein (middle). Equal loading was confirmed by Ponceau S staining (bottom).

(B) WRKY33 phosphorylation in gain-of-function *DD* seedlings after DEX treatment. Protein extracts from *DD*, *DD/wrky33/4myc-WRKY33^{WT}*, and *DD/wrky33/4myc-WRKY33^{SA}* seedlings treated with DEX (1 μ M) at various times were separated in a Phos-tag SDS-PAGE gel. After being transferred to nitrocellulose membranes, WRKY33^{WT} and WRKY33^{SA} proteins were detected by an anti-myc antibody (top). A regular immunoblot was done at the same time to detect the total WRKY33 protein (middle). Equal loading was confirmed by Ponceau S staining (bottom).

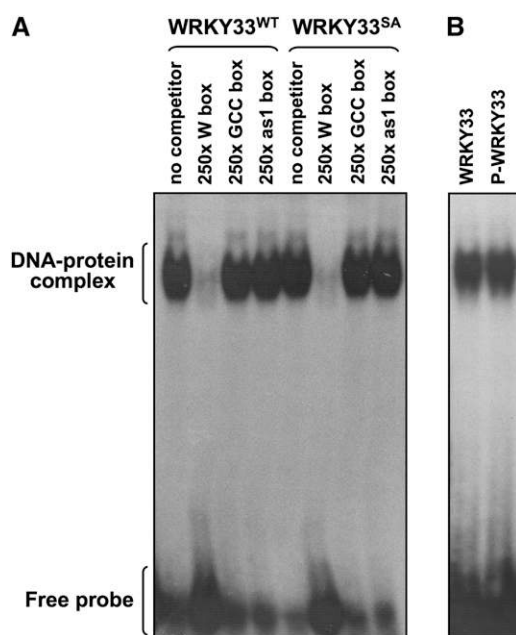


Figure 8. Phosphorylation of WRKY33 Does Not Alter Its DNA Binding Ability to the W-Box *cis*-Element.

(A) EMSA was performed using freshly prepared recombinant WRKY33^{WT} or WRKY33^{SA} protein and ³²P-labeled W-box probe. The specificity of W-box binding activity was demonstrated by competition assay using 250-fold excess unlabeled W-box, GCC-box, or as1-box DNAs.

(B) Phosphorylation of WRKY33 does not enhance its W-box binding activity. Freshly prepared recombinant WRKY33^{WT} was phosphorylated using the activated MPK3 and MPK6 (equal mixture). A control reaction without MPK3/MPK6 was processed side-by-side. The W-box binding activity of the phosphorylated and unphosphorylated (from the control reaction) was determined by EMSA as in **(A)**.

To further validate the ChIP-qPCR experiment, we quantified the enrichment of the *PAD3* promoter. Our results indicated that WRKY33 is likely to target *PAD3* genes directly and is involved in the upregulation of *PAD3* expression (Figures 1D and 2D). As shown in Figure 9B, anti-myc antibody effectively enriched the *PAD3* promoter DNA, while the control IgG failed to do so. This result is consistent with previous finding that WRKY33 directly interacts with *PAD3* promoter (Qiu et al., 2008b).

DISCUSSION

Induction of phytoalexins in plants after pathogen invasion is an integral part of induced plant disease resistance (VanEtten et al., 1989; Glazebrook et al., 1997; Hammerschmidt, 1999; Morrissey and Osbourn, 1999; Dixon, 2001). The biosynthetic pathways of a number of phytoalexins have been fully defined. However, the signaling pathways regulating their biosynthesis are largely unclear. Our previous study demonstrated that the *Arabidopsis* MPK3/MPK6 cascade is an important regulatory pathway controlling camalexin biosynthesis in *Arabidopsis* (Ren et al., 2008).

The activation of MPK3/MPK6 leads to the upregulation of the expression of camalexin biosynthetic genes, implicating the involvement of downstream transcription factors. In this report, we demonstrate that WRKY33 is a key component downstream of MPK3/MPK6 in the pathogen-induced camalexin biosynthesis. In *wrky33* mutants, both the gain-of-function MPK3/MPK6- and the pathogen-induced camalexin productions are compromised, which is associated with the loss of activation of camalexin biosynthetic genes. Genetic analysis revealed that the MAPK phosphorylation sites in WRKY33 are important for its full function/activity in vivo. Phospho-protein mobility shift assays allowed us to demonstrate the in vivo phosphorylation of WRKY33 by MPK3/MPK6 after *B. cinerea* infection. Taken together, we can conclude that WRKY33, a novel MPK3/MPK6 substrate, plays an essential role in the transcriptional activation of camalexin biosynthetic genes and camalexin induction in *Arabidopsis* in response to pathogen infection.

Dual-Level Regulation of WRKY33 by the MPK3/MPK6 Cascade in Plant Defense Response

Expression of many *WRKY* genes is highly induced by stresses, especially pathogen-related stimuli (Dong et al., 2003; Pandey and Somssich, 2009; Rushton et al., 2010). However, the signaling pathways and downstream transcription factors are unknown. Gain-of-function activation of MPK3/MPK6 was sufficient to induce *WRKY33* expression and WRKY33 protein accumulation (Figure 1F) (Wan et al., 2004), suggesting that the MPK3/MPK6 cascade might be involved in pathogen-induced *WRKY33* expression. In this report, we provide loss-of-function evidence to support this conclusion. In the *mpk3 mpk6* double mutant, *B. cinerea*-induced *WRKY33* induction was

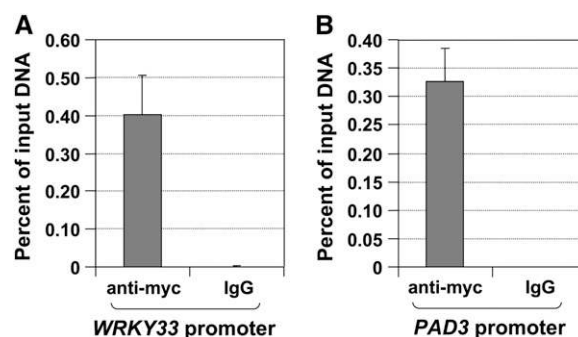


Figure 9. WRKY33 Binds to Its Own Promoter and the Promoter of *PAD3* in Vivo.

ChIP-qPCR analysis was performed using *DD/4myc-WRKY33^{WT}* plants generated from the cross of *wrky33/4myc-WRKY33^{WT}* with *DD* lines. Input chromatin was isolated from 2-week-old seedlings 12 h after DEX treatment. Epitope-tagged WRKY33-chromatin complex was immunoprecipitated with an anti-myc antibody. A control reaction was processed side-by-side using mouse IgG. ChIP- and input-DNA samples were quantified by real-time qPCR using primers specific to the promoters of *WRKY33* **(A)** and *PAD3* **(B)** genes. The ChIP results are presented as percentage of input DNA. Error bars indicate SE ($n = 3$).

compromised (Figure 3A). However, the induction of WRKY33 was not completely inhibited but rather reduced greatly, especially at earlier time points. This delayed induction of WRKY33 (Figure 3A) was associated with the blockage of camalexin induction (Ren et al., 2008). Based on these results, we conclude that, although the MPK3/MPK6 cascade plays important roles in regulating WRKY33 expression, other signaling pathways are also involved. It is also possible that the downstream signaling process involved in the induction of WRKY33 expression can still be triggered in the absence of MPK3/MPK6. Another scenario is that, in the rescued *mpk3 mpk6* double mutant, the basal level expression of MPK6 gene from the leaky DEX-inducible promoter might be able to partially compensate the mutant, although this is unlikely since we detected little/no activity from the transgenic MPK6 by the in-gel kinase activity assay in the rescued *mpk3 mpk6* double mutant after *B. cinerea* infection (Ren et al., 2008; Han et al., 2010).

W-box, the WRKY binding site, exists at high frequencies in WRKY promoters, which led to the hypothesis that WRKY transcription factors can autoactivate their own expression (Dong et al., 2003; Pandey and Somssich, 2009; Rushton et al., 2010). The WRKY33 promoter has three W-box *cis*-elements, which are required for efficient pathogen- or PAMP-triggered gene activation (Lippok et al., 2007). In the same report, it was also shown that the rapid induction of WRKY33 is independent of *de novo* protein synthesis, suggesting the involvement of post-translational regulation of a preexisting factor. In this report, we demonstrate that WRKY33 is a substrate of the stress/pathogen-inducible MPK3/MPK6, and phosphorylation of WRKY33 is likely to promote the transactivation activity of WRKY33. It is tempting to speculate that the phosphorylation of the basal-level WRKY33 protein might be involved in turning on WRKY33 expression, forming a positive feedback regulation loop. In support of this hypothesis, we found that WRKY33 interacts directly with the W-boxes in the promoter of WRKY33 based on ChIP-qPCR assay (Figure 9). The activation of WRKY33 at both transcriptional and posttranscriptional levels eventually drives the high-level activation of camalexin biosynthetic genes and the induction of camalexin biosynthesis, as depicted in our working model (Figure 10).

Camalexin Biosynthetic Enzymes and Key Regulators of the Biosynthetic Pathway Are Required for Plant Fungal Resistance

Camalexin induction plays important roles in *Arabidopsis* resistance to fungal pathogens. Mutation of key enzymes in the camalexin biosynthetic pathway compromises resistance (Glazebrook et al., 1997; Thomma et al., 1999; Zhou et al., 1999; Ferrari et al., 2003, 2007; Nafisi et al., 2007). Mutation of the *Arabidopsis* WRKY33 gene also causes enhanced susceptibility to the necrotrophic fungal pathogens *B. cinerea* and *A. brassicicola*. Ectopic overexpression of WRKY33, on the other hand, increases resistance to these two necrotrophic fungal pathogens (Zheng et al., 2006). Previously, we found that the MPK3/MPK6 cascade regulates camalexin biosynthesis and that mutation of MPK3 also compromises plant resistance to *B. cinerea* (Ren et al., 2008). In this report, we demonstrate that WRKY33 is downstream of the MPK3/MPK6 cascade in activating the expression of camalexin biosynthetic

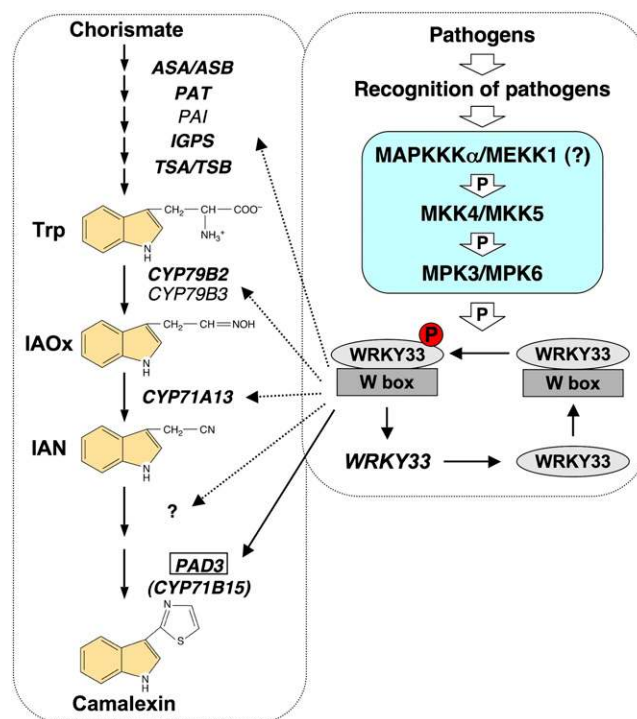


Figure 10. A Model Depicting the Involvement of WRKY33 Downstream of MPK3/MPK6 Cascade in Regulating Camalexin Biosynthesis in Plants Challenged by Pathogens.

A simplified camalexin biosynthetic pathway and its regulatory pathway are placed in separate rectangular boxes with dashed outlines. Genes whose expressions are induced by pathogen infection and MPK3/MPK6 activation are marked by bold, italic font. Arrows with solid lines are used to connect WRKY33 and its direct target genes based on ChIP-qPCR analysis. WRKY33 binds constitutively to the W-box *cis*-elements. Upon phosphorylation by MPK3/MPK6, WRKY33 is able to activate the expression of its target genes, including WRKY33, forming a potential positive feedback regulatory loop downstream of MPK3/MPK6 cascade. The activation of WRKY33 at both transcriptional and posttranslational levels eventually drives the high-level activation of camalexin biosynthetic genes and the induction of camalexin biosynthesis. One arrow may represent multiple steps because of unknown components. [See online article for color version of this figure.]

genes in response to *B. cinerea* infection. They function together in one regulatory pathway to control the expression of camalexin biosynthetic genes (Figure 10). It is likely that the compromised fungal resistance in the *wrky33* mutant is, at least in part, due to the lack of camalexin induction.

Plant sensing of *B. cinerea* invasion triggers long-lasting activation of MPK3/MPK6, which regulates WRKY33 at both transcriptional and posttranslational levels by direct phosphorylation of WRKY33 at the N-terminal Ser residues. At present, the PAMPs/effectors in *B. cinerea* and the sensors/receptors in *Arabidopsis* that trigger the long-lasting activation of the MPK3/MPK6 cascade are unknown. One of the known PAMPs from *B. cinerea*, cell wall-derived polysaccharide elicitors, only activates MPK3/MPK6 transiently (Han et al., 2010), which is not

associated with the induction of camalexin (data not shown). Prolonged activation of MPK3/MPK6 leads to the coordinated high-level induction of multiple genes in the camalexin biosynthetic pathway (Ren et al., 2008), which drives the metabolic flow from primary metabolism to the formation of camalexin, a secondary metabolite.

Is MPK4 Involved in Camalexin Induction in *Arabidopsis* Challenged by *B. cinerea*?

Our finding that WRKY33 is essential to camalexin biosynthesis is consistent with a previous report (Qiu et al., 2008b). However, more research is needed to reconcile how WRKY33 is regulated. Qiu et al. (2008b) conclude that MPK4 regulates WRKY33 by sequestering it in the MPK4/MKS1 complex in the absence of pathogens. After sensing an invading pathogen, the activation of MPK4 phosphorylates MKS1 (but not WRKY33), which releases WRKY33 from the complex so it can activate gene expression (Qiu et al., 2008b). In the conditional gain-of-function *DD Arabidopsis* plants, no MPK4 activation was detectable (Figure 1B) (Liu and Zhang, 2004; Ren et al., 2008). However, WRKY33-dependent camalexin induction was normal, suggesting that MPK4 activation is not essential to the WRKY33-dependent activation of camalexin induction. Furthermore, in the rescued *mpk3 mpk6* double mutant, high levels of MPK4 protein and activation was detected (Figure 4D) (Ren et al., 2008; Han et al., 2010), but camalexin induction by *B. cinerea* infection was compromised (Ren et al., 2008), suggesting that MPK4 activation is not sufficient to support the camalexin induction. Finally, we analyzed camalexin induction in the *mpk4* mutant and found no difference in the camalexin induction between the *mpk4* mutant and its wild-type control after *B. cinerea* infection (see Supplemental Figure 3 online). Based on these results, we conclude that MPK4 is not required for camalexin induction in *Arabidopsis* after *B. cinerea* infection. It is possible that MPK4 has differential roles in camalexin induction in response to different pathogens; for example, MPK4 is not required for the camalexin induction by a fungal pathogen (this study) but is involved in camalexin induction by a bacterial pathogen (Qiu et al., 2008b).

The Signaling Specificity of Multifunctional MPK3/MPK6 Is Conferred by Their Diverse Substrates

MPK3/MPK6 are involved in many different processes, including induction of ethylene biosynthesis in plants under stress (Kim et al., 2003; Liu and Zhang, 2004; Joo et al., 2008; Han et al., 2010), camalexin induction (Ren et al., 2008; this report), stomatal development (Wang et al., 2007; Lampard et al., 2008), flower petal abscission (Cho et al., 2008), and ovule development (Wang et al., 2008). It appears that their multifunctionality and signaling specificity are conferred by their ability to phosphorylate different substrates. Four MPK3/MPK6 substrates have been reported with functional data (Liu and Zhang, 2004; Lampard et al., 2008; Bethke et al., 2009; this report). A subset of ACS isoforms, the rate-limiting enzyme in the ethylene biosynthetic pathway, can be directly phosphorylated by MPK3 and MPK6, which stabilize the ACS protein and lead to ethylene induction

(Liu and Zhang, 2004; Joo et al., 2008; Han et al., 2010). In the stomatal pathway, phosphorylation of SPEECHLESS, a basic helix-loop-helix transcription factor involved in stomatal initiation, negatively regulates stomatal development (Lampard et al., 2008). ERF104, a member of the ethylene response factor (ERF) transcription factor family, forms a complex with MPK6. Upon MPK6 activation by flg22 PAMP treatment, ERF104 is released from the complex so it can access its target genes (Bethke et al., 2009).

Phosphorylation of WRKY33 by MPK3/MPK6 enhances its activity in promoting the expression of downstream camalexin biosynthetic genes. Different from ACS2/ACS6, accumulation of WRKY33 protein in plants after *B. cinerea* infection or in gain-of-function *DD* plants after DEX treatment is a result of transcriptional activation (Figures 1F and 2F) but not of protein stabilization. WRKY33 expressed under the 35S promoter showed no change in protein levels after *B. cinerea* infection or in *DD* background after DEX treatment (Figures 5B and 6B). As a result, MPK3/MPK6 are capable of regulating their substrates at different levels, including transcriptional activity, protein stability, and protein complex formation. In addition, the expression pattern of MPK3/MPK6 substrates can also affect signaling specificity. ACS2/ACS6, ERF104, and WRKY33 are expressed in most tissues, which is consistent with the general stress/defense responses. By contrast, SPEECHLESS is expressed only in cells about to enter the stomatal lineage, which confers the specific role of MPK3/MPK6 in plant stomatal development (Wang et al., 2007; Lampard et al., 2008). Research aimed at identifying additional MPK3/MPK6 substrates will reveal the molecular mechanisms underlying the complex roles of MPK3/MPK6 in plant growth, development, and response to environment and/or pathogens.

METHODS

Plant Growth, Treatments, Camalexin Measurement, and Statistical Analysis

Arabidopsis thaliana plants were grown under a 14-h light cycle ($100 \mu\text{E m}^{-2} \text{s}^{-1}$) at 22°C. Seedlings were grown in 20-mL gas chromatography vials with 6 mL of half-strength Murashige and Skoog liquid medium in a growth chamber under continuous light as described before (Ren et al., 2008). Two-week-old seedlings were used for experiments. Seedlings were collected at various time points after the addition of DEX or inoculation of *Botrytis cinerea* spores (4.0×10^5 spores per vial). Procedures for *B. cinerea* maintenance and spore preparation were as previously described (Ren et al., 2008; Han et al., 2010).

Camalexin production by *Arabidopsis* seedlings was determined using a previously described method (Tsuji et al., 1992; Glazebrook and Ausubel, 1994) with slight modification (Ren et al., 2008). Briefly, camalexin accumulation in the culture medium, which reflects its production in the seedlings, was quantified by fluorospectrometry with a standard curve established using known concentrations of camalexin.

At least two independent repetitions were performed for experiments with multiple time points. For single time point experiments, at least three independent repetitions were done. Results from one of the independent repeats that gave similar results were shown. $n = 3$ indicates independent biological samples from one of the repeats. Student's *t* test was used to determine whether the difference between two groups of data at a specific time point is statistically significant ($P < 0.05$). Statistically

different data groups are indicated using different number of asterisks (0 to 3) vertically placed above the columns in the graphs.

Mutant Lines and Generation of Transgenic Plants

Mutant alleles of *mpk3-1* (SALK_151594) and *mpk6-2* (Salk_073907) were used for experiments (Liu and Zhang, 2004; Wang et al., 2007). The generation of rescued *mpk3 mpk6* double mutant was detailed by Wang et al. (2007). All mutants used in this study are in the Col-0 background. Two T-DNA insertion mutant alleles, *wrky33-1* (SALK_006603) and *wrky33-2* (GABI_324B11), were described previously (Zheng et al., 2006). Both *wrky33-1* and *wrky33-2* alleles were used for experiments demonstrating the requirement of *WRKY33* in *B. cinerea*- and *DD*-induced camalexin production (Figures 1A to 1D and 2A to 2D). Similar results were obtained and results using *wrky33-1* were shown. Complementation experiments using *WRKY33-TAP*, *WRKY33^{WT}*, and *WRKY33^{SA}* transgenes (Figures 1E, 2E, and 5 to 7) were done in only *wrky33-2* background because *wrky33-1* acquired kanamycin resistance from the T-DNA insertion. For crosses, *wrky33* mutations were followed by PCR genotyping, and the *DD* transgene was followed by hygromycin resistance. F3 double homozygous seedlings were used for experiments unless stated otherwise.

For the generation of the native promoter-driven *WRKY33-TAP* (*P_{WRKY33}:WRKY33-TAP*) construct, an ~1.3-kb DNA fragment of the *WRKY33* promoter was PCR amplified from *Arabidopsis* genomic DNA using primers 5'-ATCAAGCTTCCACATATCGTGAATAAGAAACT-3' and 5'-ATCGAGCTCACGAAAAATGGAAGTTTGTATATAAAGA-3'. The promoter sequence was digested with *HindIII/SacI* and inserted into the same restriction sites to replace the cauliflower mosaic virus 35S promoter of plant transformation/expression vector pOCA30 (Chen and Chen, 2002). The full-length *WRKY33* cDNA was PCR amplified using primers 5'-ATCGAGCTCTATATGGACAATAGCAGAACAGACA-3' and 5'-ATCGGATCCGGGCATAAACGAATCGAAAAATG-3' and fused with the TAP tag as previously described (Xing and Chen, 2006). The *WRKY33-TAP* construct was then subcloned behind the *WRKY33* promoter in pOCA30. The constructs were verified by DNA sequencing.

To generate loss-of-phosphorylation *WRKY33* mutant (*WRKY33^{SA}*), we PCR amplified the wild-type *WRKY33* cDNA and cloned it into pBluescript II KS vector. Mutations were introduced by QuickChange site-directed mutagenesis (Stratagene) and confirmed by sequencing. Primers used for mutagenesis were as follows: 12AAF1, 5'-ctcctcttccatctctctcGctcctctctctgtcGctcctccactgttcc-3'; 34AAF1, 5'-ctcctccactt-gtttcGcTcctctcttttctcgtGcccctgctttgtctcc-3'; 5AF1, 5'-ctctgtaacg-tttagctGctccaaccacaggagc-3', and their complementary primers. Mutated nucleotides are marked with uppercase letters. *WRKY33^{SA}* with all five Ser residues mutated to Ala residues was generated by three successive mutagenesis steps.

To generate the *35S:4myc-WRKY33^{WT}* and *35S:4myc-WRKY33^{SA}* constructs, we amplified the wild-type and *WRKY33^{SA}* cDNA fragments using primers 5'-GGAATCCATATGGCTGCTTCTTTTCTTACAATGGA-CAATAGCAGAACCAGACA-3' and 5'-GACTAGTTCAGGGCATAAAC-GAATCG-3' and cloned the PCR fragment into a modified pBlueScript II KS vector with a 4myc epitope tag coding sequence at the 5'-end. The *WRKY33* cDNA with a 4myc epitope tag coding sequence was then moved into the *SpeI/XhoI* sites of a modified pBI121 vector.

All generated binary vectors were transformed into *Agrobacterium tumefaciens* strain GV3101. *Arabidopsis* transformation was performed by the floral dip procedure (Clough and Bent, 1998), and transformants were identified by screening for kanamycin or hygromycin resistance. Independent lines with expression of tagged *WRKY33* were identified based on RNA gel blots and/or immunoblotting analyses. From these transformants, those with a single copy of T-DNA insertion (based on the 3:1 segregation of antibiotic/herbicide resistance in T2 progeny) were isolated, and homozygote transgenic plants were further identified in the progeny based on segregation of antibiotic resistance.

Preparation of Recombinant WRKY33 Proteins and in Vitro Phosphorylation Assay

WRKY33^{WT} and *WRKY33^{SA}* cDNA was PCR amplified using primers (5'-GGAATTCATGGCTGCTTCTTTTCTTACAATG-3' and 5'-CCGCTC-GAGTCAGGGCATAAACGAATCG-3') and ligated into pET32a (+) vector in frame. The constructs were transformed into *Escherichia coli* strain BL21 (DE3). Recombinant protein expression was induced with 0.25 mM isopropylthio- β -galactoside for 3 h at 28°C. His-tagged proteins were purified using nickel columns and dialysis to 20 mM Tris-HCl, pH 7.5, overnight at 4°C.

The in vitro phosphorylation assay was performed as previously described (Liu and Zhang, 2004; Han et al., 2010). In brief, recombinant *WRKY33* proteins were mixed with activated MPK3, MPK6, MPK4, and MPK10 (20:1 substrate enzyme ratio) in the kinase reaction buffer (20 mM HEPES, pH 7.5, 10 mM MgCl₂, and 1 mM DTT) with 25 μ M ATP and [γ -³²P]-ATP (1 μ Ci per reaction). The reactions were stopped by the addition of SDS sample buffer after 30 min. Phosphorylated *WRKY33* was visualized by autoradiography after being resolved in a 10% SDS-PAGE gel.

DNA-Protein EMSA

Synthetic DNA oligonucleotide (5'-CGTTGACCGTTGACCGAGTTGACT-TTTTA-3') with three W-boxes (underlined) was used as probe. DNA probe labeling and gel mobility shift assays were performed as previously described (Kim and Zhang, 2004). Briefly, two complementary strands of the oligonucleotides were annealed and then labeled at the 5'-end using T4 polynucleotide kinase. The ³²P-labeled DNA probe was purified using Bio-Spin column (Bio-Rad). Freshly prepared recombinant *WRKY33^{WT}* or *WRKY33^{SA}* protein (1 μ g) was incubated with 20,000 to 50,000 cpm of DNA probe (2 pmole) for 30 min at room temperature in binding buffer (20 mM HEPES, pH 7.9, 0.1 μ g/ μ L herring sperm DNA, 0.5 mM DTT, 0.1 mM EDTA, and 50 mM KCl) in the presence or absence of unlabeled competitor DNA. The resulting protein-DNA complexes were resolved in 5% nondenaturing polyacrylamide gel in half-strength TBE buffer. Following electrophoresis, the gel was dried onto 3MM paper and exposed to x-ray film. For testing the effect of MAPK phosphorylation on the DNA binding activity of *WRKY33*, recombinant *WRKY33^{WT}* was first incubated with the activated MPK3 and MPK6 (equal mix) in the kinase reaction buffer with 50 μ M ATP for 60 min at room temperature before performing the EMSA assay.

Protein Extraction, Immunoblot Analysis, and in-Gel Kinase Assay

Proteins for in-gel kinase assay and immunoblot detection of Flag-tagged *DD* were extracted as previously described (Zhang and Klessig, 1997). For detection of tagged *WRKY33* proteins, total proteins were extracted using 3 volumes (v/w) of SDS-loading buffer without bromophenol blue dye (Joo et al., 2008). The concentration of protein was determined using the Bio-Rad protein assay kit with BSA as the standard. Immunoblot detection of tagged transgene products was performed as previously described (Liu and Zhang, 2004). Antibody against the myc-epitope tag was purchased from Millipore, and the anti-IgG-horseradish peroxidase (HRP) conjugate used to detect the TAP-tagged *WRKY33* was purchased from Sigma-Aldrich. MBP, *WRKY33*, or *WRKY33^{SA}* recombinant protein was used as the substrate for the in gel-kinase assay (Zhang and Klessig, 1997; Liu and Zhang, 2004).

Mobility Shift Assay to Detect in Vivo Phosphorylated Proteins

Phos-tag reagent (NARD Institute) was used for the phospho-protein mobility shift assay to detect in vivo phosphorylated *WRKY33* protein. Proteins (10 μ g) were separated in a 10% SDS-PAGE gel containing 100 μ mol/L Phos-tag and 200 μ M MnCl₂. After proteins were transferred

to a nitrocellulose membrane, 4myc-tagged WRKY33 was detected using the anti-myc antibody (Millipore).

qPCR Analysis

Total RNA was extracted using TRIzol reagent (Invitrogen). After DNase treatment, 1 µg of total RNA was used for reverse transcription. qPCR analysis was performed using an Optican 2 real-time PCR machine (MJ Research) as previously described (Ren et al., 2008). After normalization to an EF-1 α control, the relative levels of gene expression were calculated. The primer pairs (forward and backward) used for qRT-PCR were *EF1 α* (At5g60390, 5'-TGAGCAGCTCTTCTTCTTCA-3' and 5'-GGTGGTGGCATCCATCTTGTACA-3'), *CYP71A13* (At2g30770, 5'-GGGTAGAGGCTGGACCAAT-3' and 5'-ACAACCGAAGATGGA-AATGC-3'), *CYP71B15* (*PAD3*, At3g26830, 5'-GGTACGGATAAAT-CTCTATGA-3' and 5'-AGATACAGTCGATGAACCTAC-3'), *WRKY33* (At2g38470, 5'-GTGATATTGACATTCTTGACGA-3' and 5'-GATGGTTGTG-CACTTGTAGTA-3'), and *WRKY33-TAP* transgene (5'-AACACGAAA-CGCCTTCATC-3' and 5'-CGGAATTCGCCTACTTTC-3').

WRKY33 transgene expression in the *wrky33* mutant background was examined by RT-PCR using a primer pair (5'-TTCAGTCCCTCTC-TTTTCTCGAT-3' and 5'-GGTCTCCTCGTTTGGTTCTTC-3') that spans the whole open reading frame because nonfunctional transcripts are still produced from the mutated *wrky33* gene (Zheng et al., 2006). Equal cDNA input was confirmed by PCR using *EF1 α* control (5'-GATGGTCAGACCCGTGAGCACG-3' and 5'-CAGTCTCAACACGCTCCACTGGC-3'). Twenty-five cycles of PCR were performed.

ChIP-qPCR Analysis

F1 plants generated from the cross of *wrky33/4myc-WRKY33* and *DD* lines were used for ChIP assay. Two-week-old seedlings treated with 1 µM DEX for 12 h were processed as described (Kaufmann et al., 2010). Chromatin was isolated from 0.8 g of frozen tissue and sonicated with a Bioruptor sonicator (15 s on and 15 s off cycles, medium-energy settings) for 6 min. Immunoprecipitation was performed by incubating chromatin with 2 µg of anti-myc antibody (Millipore) or mouse IgG (negative control) for 1 h at 4°C. The protein-chromatin immunocomplexes were captured using Protein G-Dynal magnetic beads (Invitrogen). After Proteinase K digestion, the immunoprecipitated DNA was purified using ChIP DNA Clean and Concentrator kit (Zymo Research). Immunoprecipitated DNA and input DNA were analyzed by qPCR using primers specific for the promoter regions of *PAD3* and *WRKY33*. The primer pairs (forward and backward) used for ChIP-qPCR were *PAD3* (5'-TGTTTCATG-CACTTCTGCTCG-3' and 5'-CTTCACTGACCGAGCTAACAAA-3') and *WRKY33* (5'-TTTTGAGCAAGAGCCAAGAAT-3' and 5'-GGCTCAATG-CTTTCATCATCTT-3') that flank the W-boxes in the promoters. The ChIP results are presented as percentage of input DNA.

Accession Numbers

Sequence data from this article can be found in the Arabidopsis Genome Initiative or GenBank/EMBL databases under the following accession numbers: *MPK3* (At3g45640), *MPK6* (At2g43790), *MKK4* (At1g51660), *MKK5* (At3g21220), *EF1 α* (At5g60390), *CYP71A13* (At2g30770), *CYP71B15* (*PAD3*, At3g26830), and *WRKY33* (At2g38470).

Supplemental Data

The following materials are available in the online version of this article.

Supplemental Figure 1. Induction of *WRKY-TAP* Expression in *WRKY33-TAP/wrky33* Plants Infected by *B. cinerea*.

Supplemental Figure 2. MPK3/MPK6 Phosphorylation Sites in *WRKY33* Are Required for Full Complementation of *wrky33* Mutation.

Supplemental Figure 3. *B. cinerea*-Induced Camalexin Biosynthesis Is Not Affected by *MPK4* Mutation.

ACKNOWLEDGMENTS

We thank Melody Kroll for proofreading the manuscript. This work was supported by National Science Foundation Grants MCB-0543109 and IOS-0743957 to S.Z. and IOS-0958066 to Z.C.

Received March 9, 2011; revised March 9, 2011; accepted March 29, 2011; published April 15, 2011.

REFERENCES

- Asai, T., Tena, G., Plotnikova, J., Willmann, M.R., Chiu, W.-L., Gomez-Gomez, L., Boller, T., Ausubel, F.M., and Sheen, J. (2002). MAP kinase signalling cascade in Arabidopsis innate immunity. *Nature* **415**: 977–983.
- Ausubel, F.M. (2005). Are innate immune signaling pathways in plants and animals conserved? *Nat. Immunol.* **6**: 973–979.
- Beckers, G.J.M., Jaskiewicz, M., Liu, Y., Underwood, W.R., He, S.Y., Zhang, S., and Conrath, U. (2009). Mitogen-activated protein kinases 3 and 6 are required for full priming of stress responses in *Arabidopsis thaliana*. *Plant Cell* **21**: 944–953.
- Bethke, G., Unthan, T., Uhrig, J.F., Pöschl, Y., Gust, A.A., Scheel, D., and Lee, J. (2009). Flg22 regulates the release of an ethylene response factor substrate from MAP kinase 6 in *Arabidopsis thaliana* via ethylene signaling. *Proc. Natl. Acad. Sci. USA* **106**: 8067–8072.
- Boller, T. (2005). Peptide signalling in plant development and self/non-self perception. *Curr. Opin. Cell Biol.* **17**: 116–122.
- Böttcher, C., Westphal, L., Schmotz, C., Prade, E., Scheel, D., and Glawischig, E. (2009). The multifunctional enzyme CYP71B15 (PHYTOALEXIN DEFICIENT3) converts cysteine-indole-3-acetonitrile to camalexin in the indole-3-acetonitrile metabolic network of *Arabidopsis thaliana*. *Plant Cell* **21**: 1830–1845.
- Broekaert, W.F., Delauré, S.L., De Bolle, M.F.C., and Cammue, B.P.A. (2006). The role of ethylene in host-pathogen interactions. *Annu. Rev. Phytopathol.* **44**: 393–416.
- Chen, C., and Chen, Z. (2002). Potentiation of developmentally regulated plant defense response by AtWRKY18, a pathogen-induced Arabidopsis transcription factor. *Plant Physiol.* **129**: 706–716.
- Cho, S.K., Larue, C.T., Chevalier, D., Wang, H., Jinn, T.-L., Zhang, S., and Walker, J.C. (2008). Regulation of floral organ abscission in *Arabidopsis thaliana*. *Proc. Natl. Acad. Sci. USA* **105**: 15629–15634.
- Clough, S.J., and Bent, A.F. (1998). Floral dip: A simplified method for *Agrobacterium*-mediated transformation of *Arabidopsis thaliana*. *Plant J.* **16**: 735–743.
- Cui, H., Wang, Y., Xue, L., Chu, J., Yan, C., Fu, J., Chen, M., Innes, R.W., and Zhou, J.-M. (2010). *Pseudomonas syringae* effector protein AvrB perturbs Arabidopsis hormone signaling by activating MAP kinase 4. *Cell Host Microbe* **7**: 164–175.
- Dangl, J.L., and Jones, J.D.G. (2001). Plant pathogens and integrated defence responses to infection. *Nature* **411**: 826–833.
- del Pozo, O., Pedley, K.F., and Martin, G.B. (2004). MAPKKKalpha is a positive regulator of cell death associated with both plant immunity and disease. *EMBO J.* **23**: 3072–3082.
- Dixon, R.A. (2001). Natural products and plant disease resistance. *Nature* **411**: 843–847.
- Dong, J., Chen, C., and Chen, Z. (2003). Expression profiles of the Arabidopsis WRKY gene superfamily during plant defense response. *Plant Mol. Biol.* **51**: 21–37.

- Ferrari, S., Galletti, R., Denoux, C., De Lorenzo, G., Ausubel, F.M., and Dewdney, J.** (2007). Resistance to *Botrytis cinerea* induced in *Arabidopsis* by elicitors is independent of salicylic acid, ethylene, or jasmonate signaling but requires PHYTOALEXIN DEFICIENT3. *Plant Physiol.* **144**: 367–379.
- Ferrari, S., Plotnikova, J.M., De Lorenzo, G., and Ausubel, F.M.** (2003). *Arabidopsis* local resistance to *Botrytis cinerea* involves salicylic acid and camalexin and requires EDS4 and PAD2, but not SID2, EDS5 or PAD4. *Plant J.* **35**: 193–205.
- Glazebrook, J., and Ausubel, F.M.** (1994). Isolation of phytoalexin-deficient mutants of *Arabidopsis thaliana* and characterization of their interactions with bacterial pathogens. *Proc. Natl. Acad. Sci. USA* **91**: 8955–8959.
- Glazebrook, J., Zook, M., Mert, F., Kagan, I., Rogers, E.E., Crute, I.R., Holub, E.B., Hammerschmidt, R., and Ausubel, F.M.** (1997). Phytoalexin-deficient mutants of *Arabidopsis* reveal that PAD4 encodes a regulatory factor and that four PAD genes contribute to downy mildew resistance. *Genetics* **146**: 381–392.
- Hammerschmidt, R.** (1999). Phytoalexins: What have we learned after 60 years? *Annu. Rev. Phytopathol.* **37**: 285–306.
- Han, L., Li, G.J., Yang, K.Y., Mao, G., Wang, R., Liu, Y., and Zhang, S.** (2010). Mitogen-activated protein kinase 3 and 6 regulate *Botrytis cinerea*-induced ethylene production in *Arabidopsis*. *Plant J.* **64**: 114–127.
- Ichimura, K., et al; MAPK Group.** (2002). Mitogen-activated protein kinase cascades in plants: A new nomenclature. *Trends Plant Sci.* **7**: 301–308.
- Jin, H., Liu, Y., Yang, K.-Y., Kim, C.Y., Baker, B., and Zhang, S.** (2003). Function of a mitogen-activated protein kinase pathway in *N* gene-mediated resistance in tobacco. *Plant J.* **33**: 719–731.
- Joo, S., Liu, Y., Lueth, A., and Zhang, S.** (2008). MAPK phosphorylation-induced stabilization of ACS6 protein is mediated by the non-catalytic C-terminal domain, which also contains the cis-determinant for rapid degradation by the 26S proteasome pathway. *Plant J.* **54**: 129–140.
- Kaufmann, K., Muñio, J.M., Østerås, M., Farinelli, L., Krajewski, P., and Angenent, G.C.** (2010). Chromatin immunoprecipitation (ChIP) of plant transcription factors followed by sequencing (ChIP-SEQ) or hybridization to whole genome arrays (ChIP-CHIP). *Nat. Protoc.* **5**: 457–472.
- Kim, C.Y., Liu, Y., Thorne, E.T., Yang, H., Fukushige, H., Gassmann, W., Hildebrand, D., Sharp, R.E., and Zhang, S.** (2003). Activation of a stress-responsive mitogen-activated protein kinase cascade induces the biosynthesis of ethylene in plants. *Plant Cell* **15**: 2707–2718.
- Kim, C.Y., and Zhang, S.** (2004). Activation of a mitogen-activated protein kinase cascade induces WRKY family of transcription factors and defense genes in tobacco. *Plant J.* **38**: 142–151.
- Kroj, T., Rudd, J.J., Nürnberger, T., Gäbler, Y., Lee, J., and Scheel, D.** (2003). Mitogen-activated protein kinases play an essential role in oxidative burst-independent expression of pathogenesis-related genes in parsley. *J. Biol. Chem.* **278**: 2256–2264.
- Lampard, G.R., Macalister, C.A., and Bergmann, D.C.** (2008). *Arabidopsis* stomatal initiation is controlled by MAPK-mediated regulation of the bHLH SPEECHLESS. *Science* **322**: 1113–1116.
- Lippok, B., Birkenbihl, R.P., Rivory, G., Brümmer, J., Schmelzer, E., Logemann, E., and Somssich, I.E.** (2007). Expression of AtWRKY33 encoding a pathogen- or PAMP-responsive WRKY transcription factor is regulated by a composite DNA motif containing W box elements. *Mol. Plant Microbe Interact.* **20**: 420–429.
- Liu, Y., Ren, D., Pike, S., Pallardy, S., Gassmann, W., and Zhang, S.** (2007). Chloroplast-generated reactive oxygen species are involved in hypersensitive response-like cell death mediated by a mitogen-activated protein kinase cascade. *Plant J.* **51**: 941–954.
- Liu, Y., and Zhang, S.** (2004). Phosphorylation of 1-aminocyclopropane-1-carboxylic acid synthase by MPK6, a stress-responsive mitogen-activated protein kinase, induces ethylene biosynthesis in *Arabidopsis*. *Plant Cell* **16**: 3386–3399.
- Martin, G.B., Bogdanove, A.J., and Sessa, G.** (2003). Understanding the functions of plant disease resistance proteins. *Annu. Rev. Plant Biol.* **54**: 23–61.
- Menke, F.L.H., van Pelt, J.A., Pieterse, C.M.J., and Klessig, D.F.** (2004). Silencing of the mitogen-activated protein kinase MPK6 compromises disease resistance in *Arabidopsis*. *Plant Cell* **16**: 897–907.
- Morrissey, J.P., and Osbourn, A.E.** (1999). Fungal resistance to plant antibiotics as a mechanism of pathogenesis. *Microbiol. Mol. Biol. Rev.* **63**: 708–724.
- Nafisi, M., Goregaoker, S., Botanga, C.J., Glawischnig, E., Olsen, C.E., Halkier, B.A., and Glazebrook, J.** (2007). *Arabidopsis* cytochrome P450 monooxygenase 71A13 catalyzes the conversion of indole-3-acetaldoxime in camalexin synthesis. *Plant Cell* **19**: 2039–2052.
- Nakagami, H., Pitzschke, A., and Hirt, H.** (2005). Emerging MAP kinase pathways in plant stress signalling. *Trends Plant Sci.* **10**: 339–346.
- Nürnberger, T., and Scheel, D.** (2001). Signal transmission in the plant immune response. *Trends Plant Sci.* **6**: 372–379.
- Pandey, S.P., and Somssich, I.E.** (2009). The role of WRKY transcription factors in plant immunity. *Plant Physiol.* **150**: 1648–1655.
- Petersen, M., et al.** (2000). *Arabidopsis* map kinase 4 negatively regulates systemic acquired resistance. *Cell* **103**: 1111–1120.
- Qiu, J.-L., et al.** (2008b). *Arabidopsis* MAP kinase 4 regulates gene expression through transcription factor release in the nucleus. *EMBO J.* **27**: 2214–2221.
- Qiu, J.-L., Zhou, L., Yun, B.-W., Nielsen, H.B., Fiiil, B.K., Petersen, K., Mackinlay, J., Loake, G.J., Mundy, J., and Morris, P.C.** (2008a). *Arabidopsis* mitogen-activated protein kinase kinases MKK1 and MKK2 have overlapping functions in defense signaling mediated by MEK1, MPK4, and MKS1. *Plant Physiol.* **148**: 212–222.
- Ren, D., Liu, Y., Yang, K.-Y., Han, L., Mao, G., Glazebrook, J., and Zhang, S.** (2008). A fungal-responsive MAPK cascade regulates phytoalexin biosynthesis in *Arabidopsis*. *Proc. Natl. Acad. Sci. USA* **105**: 5638–5643.
- Ren, D., Yang, H., and Zhang, S.** (2002). Cell death mediated by MAPK is associated with the hydrogen peroxide production in *Arabidopsis*. *J. Biol. Chem.* **277**: 559–565.
- Rushton, P.J., Somssich, I.E., Ringler, P., and Shen, Q.J.** (2010). WRKY transcription factors. *Trends Plant Sci.* **15**: 247–258.
- Schuhegger, R., Nafisi, M., Mansourova, M., Petersen, B.L., Olsen, C.E., Svatos, A., Halkier, B.A., and Glawischnig, E.** (2006). CYP71B15 (PAD3) catalyzes the final step in camalexin biosynthesis. *Plant Physiol.* **141**: 1248–1254.
- Staskawicz, B.J., Ausubel, F.M., Baker, B.J., Ellis, J.G., and Jones, J.D.G.** (1995). Molecular genetics of plant disease resistance. *Science* **268**: 661–667.
- Suarez-Rodriguez, M.C., Adams-Phillips, L., Liu, Y., Wang, H., Su, S.-H., Jester, P.J., Zhang, S., Bent, A.F., and Krysan, P.J.** (2007). MEK1 is required for flg22-induced MPK4 activation in *Arabidopsis* plants. *Plant Physiol.* **143**: 661–669.
- Tena, G., Asai, T., Chiu, W.-L., and Sheen, J.** (2001). Plant mitogen-activated protein kinase signaling cascades. *Curr. Opin. Plant Biol.* **4**: 392–400.
- Thomma, B.P.H.J., Nelissen, I., Eggermont, K., and Broekaert, W.F.** (1999). Deficiency in phytoalexin production causes enhanced susceptibility of *Arabidopsis thaliana* to the fungus *Alternaria brassicicola*. *Plant J.* **19**: 163–171.
- Tsuji, J., Jackson, E.P., Gage, D.A., Hammerschmidt, R., and Somerville, S.C.** (1992). Phytoalexin accumulation in *Arabidopsis thaliana* during the hypersensitive reaction to *Pseudomonas syringae* pv *syringae*. *Plant Physiol.* **98**: 1304–1309.

- VanEtten, H.D., Matthews, D.E., and Matthews, P.S.** (1989). Phytoalexin detoxification: Importance for pathogenicity and practical implications. *Annu. Rev. Phytopathol.* **27**: 143–164.
- van Loon, L.C., Geraats, B.P.J., and Linthorst, H.J.M.** (2006). Ethylene as a modulator of disease resistance in plants. *Trends Plant Sci.* **11**: 184–191.
- Wan, J., Zhang, S., and Stacey, G.** (2004). Activation of a mitogen-activated protein kinase pathway in *Arabidopsis* by chitin. *Mol. Plant Pathol.* **5**: 125–135.
- Wang, H., Liu, Y., Bruffett, K., Lee, J., Hause, G., Walker, J.C., and Zhang, S.** (2008). Haplo-insufficiency of MPK3 in MPK6 mutant background uncovers a novel function of these two MAPKs in *Arabidopsis* ovule development. *Plant Cell* **20**: 602–613.
- Wang, H., Ngwenyama, N., Liu, Y., Walker, J.C., and Zhang, S.** (2007). Stomatal development and patterning are regulated by environmentally responsive mitogen-activated protein kinases in *Arabidopsis*. *Plant Cell* **19**: 63–73.
- Xing, D., and Chen, Z.** (2006). Effects of mutations and constitutive overexpression of EDS1 and PAD4 on plant resistance to different types of microbial pathogens. *Plant Sci.* **171**: 251–262.
- Yang, K.-Y., Liu, Y., and Zhang, S.** (2001). Activation of a mitogen-activated protein kinase pathway is involved in disease resistance in tobacco. *Proc. Natl. Acad. Sci. USA* **98**: 741–746.
- Zhang, J., et al.** (2007). A *Pseudomonas syringae* effector inactivates MAPKs to suppress PAMP-induced immunity in plants. *Cell Host Microbe* **1**: 175–185.
- Zhang, S., and Klessig, D.F.** (1997). Salicylic acid activates a 48-kD MAP kinase in tobacco. *Plant Cell* **9**: 809–824.
- Zhang, S., and Klessig, D.F.** (2001). MAPK cascades in plant defense signaling. *Trends Plant Sci.* **6**: 520–527.
- Zheng, Z., Qamar, S.A., Chen, Z., and Mengiste, T.** (2006). *Arabidopsis* WRKY33 transcription factor is required for resistance to necrotrophic fungal pathogens. *Plant J.* **48**: 592–605.
- Zhou, N., Tootle, T.L., and Glazebrook, J.** (1999). *Arabidopsis* PAD3, a gene required for camalexin biosynthesis, encodes a putative cytochrome P450 monooxygenase. *Plant Cell* **11**: 2419–2428.